NANO LETTERS

Letter

pubs.acs.org/NanoLett

Comparing Graphene Growth on Cu(111) versus Oxidized Cu(111)

Stefano Gottardi,*[,†] Kathrin Müller,[†] Luca Bignardi,[†] Juan Carlos Moreno-López,[†] Tuan Anh Pham,[†] Oleksii Ivashenko,[†] Mikhail Yablonskikh,[‡] Alexei Barinov,[‡] Jonas Björk,[§] Petra Rudolf,[†] and Meike Stöhr*[,†]

[†]Zernike Institute for Advanced Materials, University of Groningen, Nijenborgh 4, 9747 AG Groningen, The Netherlands

[‡]Sincrotrone Trieste s.c.p.a., 34149 Basovizza, Trieste, Italy

[§]Department of Physics, Chemistry, and Biology, IFM, Linköping University, 58183 Linköping, Sweden

Supporting Information

ABSTRACT: The epitaxial growth of graphene on catalytically active metallic surfaces via chemical vapor deposition (CVD) is known to be one of the most reliable routes toward high-quality large-area graphene. This CVD-grown graphene is generally coupled to its metallic support resulting in a modification of its intrinsic properties. Growth on oxides is a promising alternative that might lead to a decoupled graphene layer. Here, we compare graphene on a pure metallic to graphene on an oxidized copper surface in both cases grown by a single step CVD process under similar conditions. Remarkably, the growth on copper oxide, a high-k dielectric material, preserves the intrinsic properties of graphene; it is not doped and a linear dispersion is observed close to the Fermi energy. Density functional theory calculations give additional insight into the reaction processes and help explaining the catalytic activity of the copper oxide surface.

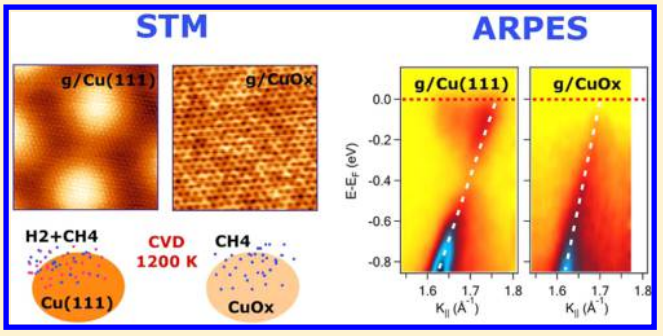

KEYWORDS: *Graphene, copper oxide, dielectric, catalysis, electronic properties, ARPES, STM*

Graphene, a single layer of carbon atoms, is supposed to transcend conventional silicon-based electronics, because of its overwhelming electronic properties.[1−4] However, a scalable and versatile route to obtain high quality graphene on noninteracting substrates that also preserves graphene's intrinsic properties, a prerequisite for graphene electronic devices,[3,4] has not been developed yet. In comparison to the established chemical vapor deposition (CVD) growth on metals,[5−7] the epitaxial growth of graphene on both noninteracting and high-k dielectric substrates like oxides, is a significant challenge that is gaining increasing interest.[8−12] Direct growth on a dielectric material will eliminate the transfer step otherwise required to obtain freestanding-like graphene[2] on a (nearly) noninteracting substrate. The transfer step is not easily scalable and often reduces the graphene quality by introducing defects and contaminations. For this reason, various alternative routes have been developed.[13−19] However, the desired but still most challenging fabrication route is a single-step and self-limiting growth process directly on high-k dielectric substrates that preserves the intrinsic properties of graphene.

Metal oxides are promising candidates in this respect due to their good dielectric and catalytic properties.[20] In general, graphene grown on nonmetallic surfaces like oxides exhibits reduced quality in comparison to graphene grown on metals[8] and in some cases graphene was even found to be either p- or n-doped.[9,21] Only very recently, high quality graphene growth on $SrTiO_3$ was achieved[10] demonstrating that this is a viable and promising alternative. Moreover, evidence of graphene growth on the oxygen-induced reconstructed copper surface was reported in the case of copper films.[11]

Here we compare the growth of graphene on a high purity oxide-free Cu(111) single crystal with the growth on a Cu(111) single crystal after the creation of a thin oxide layer. We also performed density functional theory (DFT) calculations to get insight into the reaction processes and help explaining the catalytic activity of copper oxide.

Our results demonstrate the feasibility of growing high-quality monolayer graphene by a one-step growth process on a preoxidized Cu(111) surface. In contrast to graphene on Cu(111), where a weak interaction and doping are found,[22] graphene grown on the oxidized Cu surface is effectively decoupled from its substrate and thereby its intrinsic properties are preserved. Importantly, this implies that the band structure of freestanding graphene is retained, where doping is absent. Because copper oxide is a high-k dielectric material, these findings constitute an important contribution toward the realization of graphene-based electronic devices. Moreover, we provide crucial information for the clarification of the role of

Received: September 23, 2014
Revised: January 9, 2015
Published: January 22, 2015

DOI: 10.1021/nl5036463
Nano Lett. 2015, 15, 917−922

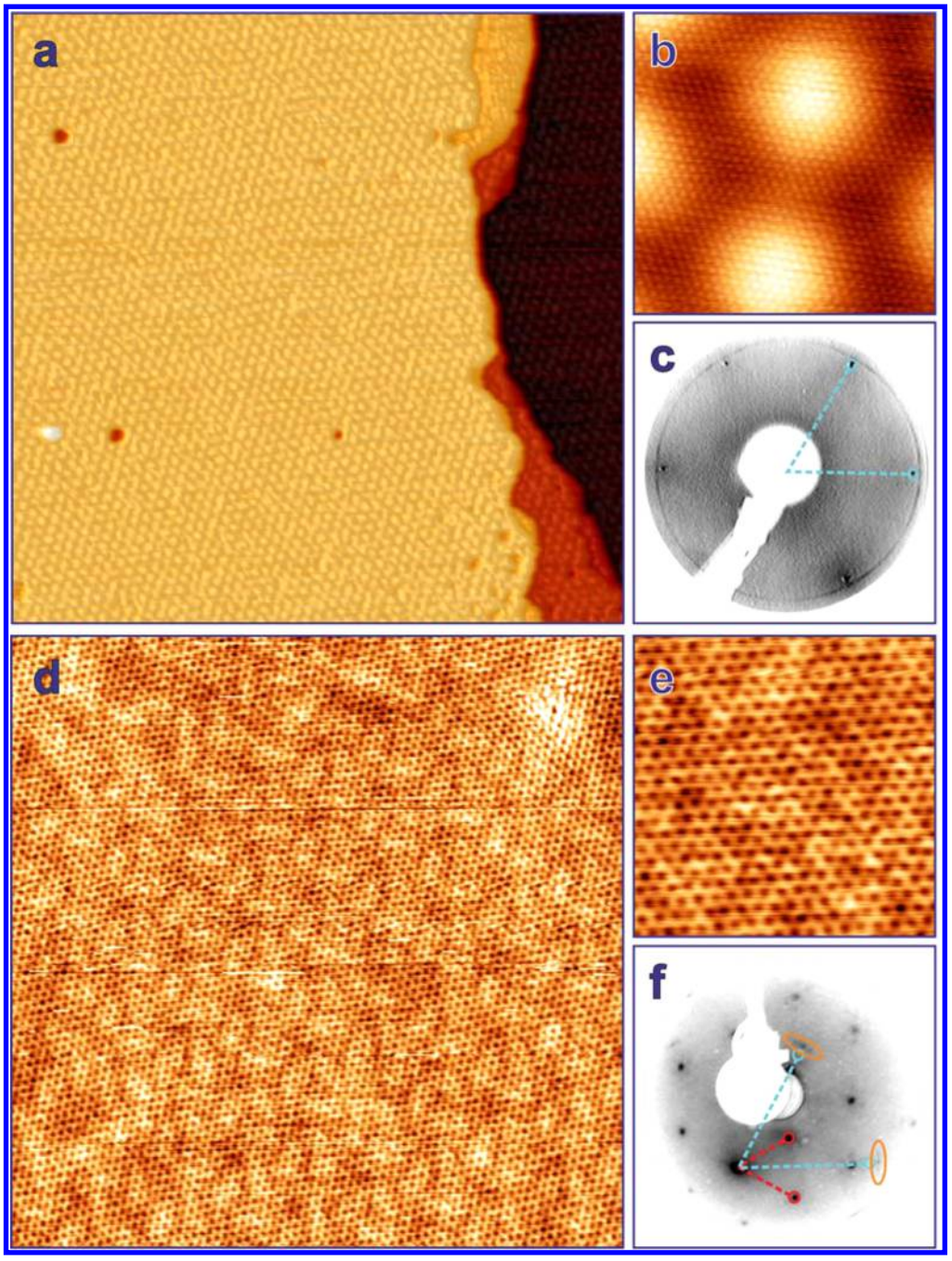

Figure 1. Structural characterization of graphene grown on Cu(111) and on oxidized Cu(111). (a) STM image (170 nm × 170 nm) for graphene grown on Cu(111). A Moiré pattern arising due to the lattice mismatch between graphene and Cu(111) is visible that continues over the step edges. (b) STM image (6.8 nm × 6.8 nm) showing atomic resolution with the Moiré pattern present in the background. (c) LEED pattern of graphene grown on Cu(111) taken at a primary energy of 150 eV. In addition to the Cu(111) diffraction spots (lattice vectors in light blue), a ring surrounding these spots is visible that is related to the presence of graphene. (d) STM image (17 nm × 17 nm) of graphene grown on oxidized Cu(111). A diffuse background coming from the oxide is visible. (e) STM image for graphene grown on oxidized Cu(111) (4.3 nm × 4.3 nm) showing atomic resolution. (f) LEED pattern of graphene grown on oxidized Cu(111) taken at a primary energy of 61 eV. The high intensity diffraction spots arise from the oxidized Cu(111) (lattice vectors in red) while the spots marked in orange indicate the presence of graphene (see also Figure 2a,b).

oxygen and of the surface oxide for CVD growth of graphene on copper, a topic recently subject to much discussion.[23−28] Because the (111)-oriented facets of polycrystalline Cu substrates are known to promote fast, high-quality monolayer graphene growth,[29] our results for single crystal Cu(111) surfaces will be also relevant for polycrystalline substrates.

For graphene growth on Cu(111), the Cu single crystal was preannealed in a hydrogen atmosphere to guarantee an oxide-free metallic surface. For graphene growth on oxidized Cu(111), the clean copper single crystal was exposed to air for approximately 12 h to obtain an oxidized surface onto which graphene was grown subsequently without any hydrogen treatment (see Supporting Information Methods and S1 for more details).

The structural properties of graphene were characterized by scanning tunneling microscopy (STM) as well as by low energy

DOI: 10.1021/nl5036463
Nano Lett. 2015, 15, 917−922

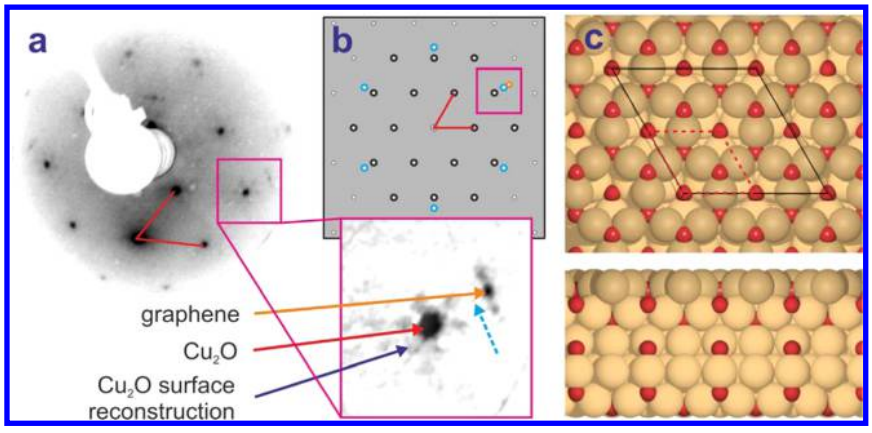

Figure 2. (a) LEED pattern of graphene grown on oxidized Cu(111), incident electron energy $E = 61$ eV. The oxide diffraction spots are much more intense than the Cu(111) spots, which are at this particular energy not visible. The Cu_2O reciprocal unit cell vectors are marked in red. Pink square: close-up view of a second order Cu_2O spot enhanced with a derivative algorithm for better visibility. The spots arising from Cu_2O (red arrow), graphene (orange arrow), and the Cu_2O surface reconstruction (violet arrow) are marked. The blue dashed arrow points to the position where the Cu(111) diffraction spot would be expected. (b) Simulated LEED pattern of Cu_2O on Cu(111), in bold (black) the strongest diffraction spots of the oxide are marked. The Cu(111) diffraction spots are indicated with blue circles. The expected location of the graphene diffraction spot is marked by an orange circle. (c) Model of the $Cu_2O(111)$ surface. Red, oxygen atoms; brown, Cu atoms. The top layer Cu atoms are represented by darker colors. Top: top view. Unit cell marked in red, $p(2 \times 2)$ superstructure used for DFT calculations indicated by black lines. Bottom: side view.

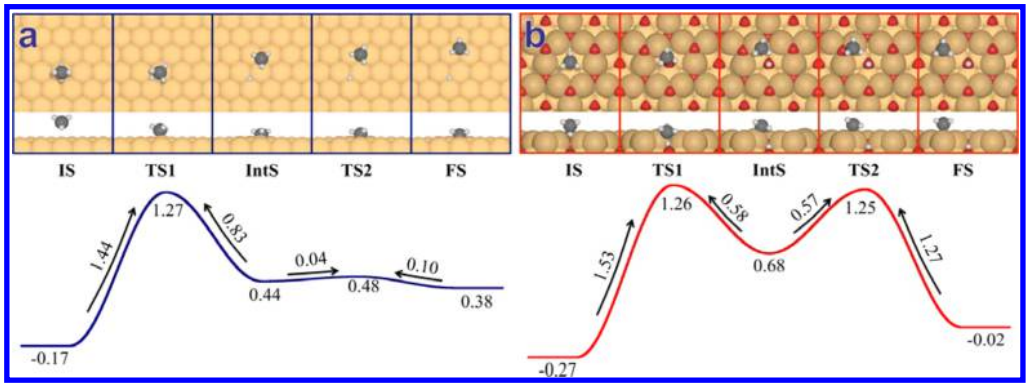

Figure 3. Mechanism of methane dissociation on Cu(111) (a) and $Cu_2O(111)$ (b) from DFT-based transition state calculations. The energies are given with respect to the reference system of the free surface and methane in gas phase in units of eV. Furthermore, the barrier heights for overcoming the different transition states are indicated. For both surfaces, the first step with transition state TS1 is associated with dehydrogenation, while the second step with transition state TS2 is associated with CH_3 diffusion.

electron diffraction (LEED). In Figure 1, STM images and LEED patterns of graphene on both metallic Cu(111) and oxidized Cu(111) are shown. On Cu(111), graphene grows over the Cu step edges, which is confirmed by the absence of changes in the Moiré patterns[30] originating from the lattice mismatch between graphene and Cu(111) (Figure 1a). A close-up view of graphene on Cu(111) is reported in Figure 1b, where in addition to the Moiré pattern the graphene lattice is visible. In different areas of the sample diverse periodicities for the Moiré patterns were observed depending on the specific angles between the principal directions of graphene and Cu(111). In the LEED pattern (Figure 1c) this polycrystalline character of graphene is mirrored in a circle around the first order Cu(111) diffraction spots.

For graphene grown on oxidized Cu(111), in addition to the clearly visible atomic honeycomb lattice of graphene, a background due to the thin oxide layer is observed (Figure 1d,e). A change of the tunneling or tip conditions sometimes results in contrast variations (Supporting Information Figure 5−6 and S4). Importantly, the STM images show that high quality (defect-free) graphene can be grown on the oxidized copper surface. As compared to graphene on the pure metal surface, the LEED pattern of graphene on oxidized Cu(111) (Figures 1f and 2a,b) shows additional diffraction spots (marked in red) due to the presence of the Cu surface oxide. Analysis of the LEED pattern yields that the surface oxide is mainly arranged in a Cu_2O lattice[31,32] that is known to reconstruct by removing the under-coordinated Cu atoms of the top atomic layer[31] (see Figure 2c and Supporting Information Figure 3). The Cu(111) first order diffraction spots are barely visible because of the presence of the oxide layer. A LEED pattern where the Cu(111) diffraction spots becomes visible is shown in Supporting Information Figure 4c. The circular feature observed in LEED patterns for graphene on metallic Cu(111) is replaced by individual diffraction spots, mainly located along the principal Cu directions and next to the Cu diffraction spots (orange ovals in Figure 1f, orange markers in Figure 2a,b). This indicates a substantial decrease of rotational disorder of the graphene domains. There is also evidence for a long-range ordered structure with a periodicity of about 3.1 nm (indicated in violet in Figure 2a), which is attributed to a reconstruction due to the lattice mismatch of the oxide layer with the Cu(111) surface and with graphene.

DOI: 10.1021/nl5036463
Nano Lett. 2015, 15, 917−922

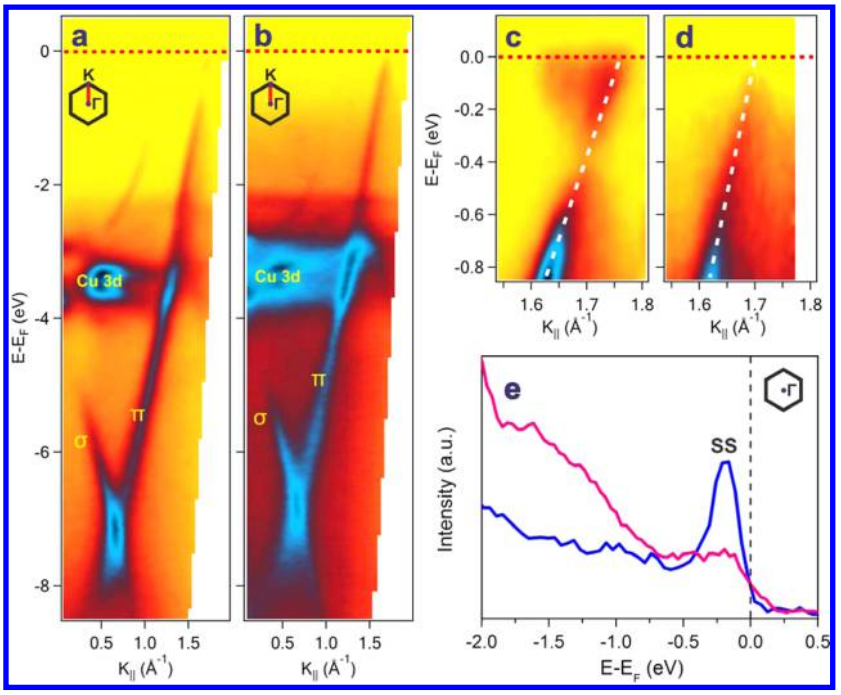

Figure 4. Comparison of the electronic properties of graphene grown on Cu(111) and on oxidized Cu(111). Energy dispersion curves along the $\overline{\Gamma K}$ direction of the graphene Brillouin zone (inset) for graphene grown on Cu(111) (a) and oxidized Cu(111) (b), respectively. The Cu 3d as well as the σ- and π-bands of graphene are labeled in yellow. Detail of the Dirac cone at the K-point of the graphene Brillouin zone for graphene grown on Cu(111) (c) and on oxidized Cu(111) (d), respectively. The white dashed line indicates the linear dispersion of the Dirac cone. (e) Normal emission spectra measured at the Γ-point of the graphene Brillouin zone for graphene on Cu(111) (blue) and on oxidized Cu(111) (pink), respectively. The Cu(111) surface state (SS) is shifted toward the Fermi energy for graphene grown on Cu(111) while it is not present anymore for graphene grown on oxidized Cu(111).

Among the ordered oxide structures observed in LEED and STM, Cu_2O was by far the most abundant; for this reason we performed DFT calculations using this Cu oxide as a model surface. However, a second ordered oxide was in rare cases found to coexist on the surface (see Supporting Information S3 for details).

Before going into the details of how graphene grows on the oxidized Cu surface, we recall that dehydrogenation of the carbon precursor (in our case methane) is the rate limiting step for graphene growth by CVD,[33] and that it was recently shown that small amounts of oxygen on the copper surface can enhance the dehydrogenation.[28] To understand how the dehydrogenation proceeds on the copper oxide surface compared to metallic Cu(111), we calculated the energy barrier for methane dehydrogenation on both Cu(111) and Cu_2O(111) within the framework of DFT including van der Waals interactions (see Supporting Information Methods). The reaction energy profiles, along with side- and top-views of the optimized adsorption geometries, are reported in Figure 3.

Surprisingly, the energy barrier for methane dehydrogenation on the Cu_2O(111) surface is only slightly higher (1.53 eV) than on a metallic Cu(111) surface (1.44 eV). Furthermore, as methane binds slightly stronger to Cu_2O(111) than to Cu(111) by 0.10 eV, the relative ratio between methane dissociation and desorption (given by the Boltzmann factor) becomes very similar on both surfaces. This elucidates why graphene can form on both surfaces under similar growth conditions.

Previous studies showed that the top atomic layer of the Cu_2O(111) surface spontaneously forms a network of vacancies[31] (Figures 2c and 3) resulting in a reconstruction, which, according to our DFT calculations, act as catalytic centers for dehydrogenation. Methane is trapped at a Cu vacancy on top of an undercoordinated oxygen atom, which catalyzes the dehydrogenation to form an −OH and a CH_3 group. The CH_3 then diffuses to a free oxygen atom in the top layer or reacts with other molecules forming graphene. Notably, the DFT results indicate that CH_3 diffusion is considerably slower on Cu_2O(111) than on Cu(111). This may be the rate-limiting factor for the growth on the oxidized surface. Assuming that the same growth conditions are used, fewer graphene domains should be obtained on Cu_2O(111) as compared to Cu(111). These results are consistent with recent studies, which have shown that small amounts of oxygen on a copper surface alter the growth from an edge-attachment-limited to a diffusion-limited process, reducing the graphene nucleation density.[27,28]

Our DFT calculations give an overview of the main steps involved in the methane dehydrogenation process. However, to fully model the complex kinetics of graphene growth at high temperatures a more comprehensive theoretical study would be required, taking into account many other processes, such as the recombination of two CH_3 molecules and the attachment of CH_3 to the graphene domains at elevated temperatures. However, this would require a significant additional computational effort, clearly beyond the scope of this study. Because local defects and vacancies are expected to only enhance the surface reactivity with respect to the model presented here, this will not change our main conclusion. Indeed, due to the relatively high oxygen mobility in copper oxides, especially at the high growth temperatures (>1200 K), vacancies can be easily created and may act as additional catalytic centers. At the same time, oxygen ions from deeper layers can migrate to the surface and compensate for the surface reduction that might happen during graphene growth. We speculate that this

DOI: 10.1021/nl5036463
Nano Lett. 2015, 15, 917−922

remarkable flexibility of the oxide layer may be the key factor for obtaining high quality (defect-free) graphene on copper oxide.

Although the high oxygen mobility on the copper oxide layer plays an important role in vacancy creation and annihilation, the oxide layer itself is quite stable. Indeed the oxide layer is easily preserved upon annealing to 1200 K in ultrahigh vacuum (UHV) and can be removed only by several cycles of sputtering and annealing. Moreover our experiments exclude the possibility of oxygen migration from the bulk that is instead observed for low purity copper foil.

The oxide layer has a dramatic effect on the electronic coupling between graphene and the substrate as revealed by angle-resolved photoemission spectroscopy (ARPES) measurements (see Supporting Information S2 for more information), performed to investigate the electronic structure of graphene grown on both metallic and oxidized Cu(111). ARPES spectra were acquired along the $\overline{\Gamma K}$ direction of the graphene Brillouin zone with a photon energy of 27 eV. Figure 4 shows the comparison of the ARPES measurements for graphene grown on metallic (a,c) and on oxidized (b,d) Cu(111). The 3d-bands of copper are visible between 2 and 4 eV below the Fermi energy, E_F, while the π-band of graphene is present between E_F and ~8.5 eV below E_F (Figure 4a,b). Graphene grown on metallic copper is n-type doped with the Dirac energy residing at about 0.38 eV below E_F (Figure 4c). The $\pi-\pi^*$ and σ-bands are shifted accordingly. Such n-type doping is in agreement with theoretical predictions and previous experimental reports.[5,22,34,35] On the other hand, for graphene grown on oxidized Cu(111) the σ- and π-bands are located closer to E_F than for graphene on metallic Cu(111) (Figure 4b). This becomes more evident when inspecting the Dirac cone (Figure 4d). Notably, within the limit of our experimental resolution (~25 meV), the Dirac points reside at E_F, which means that graphene grown on oxidized Cu(111) is not doped and the oxide effectively decouples graphene from its metallic support.

For weakly interacting graphene, the Fermi velocity can be approximated by fitting the dispersion of the π-band close to the Dirac points with a Dirac-like linear dispersion.[1] Graphene grown on copper oxide is found to have a Fermi velocity of $\sim 1.4 \times 10^6$ m/s, which is in agreement with the theoretically predicted value of freestanding graphene.[1] For graphene grown on metallic Cu(111), a nearly three times smaller Fermi velocity of $\sim 0.5 \times 10^6$ m/s is obtained. The presence of electronic coupling for graphene on Cu(111) is also evidenced by a shift of the Shockley surface state of Cu(111) toward the Fermi energy (Figure 4e and Supporting Information Figure 2). The bottom of the parabolic dispersion of the surface state is shifted from its usual value of 0.4 eV below E_F for Cu(111) to about 0.23 eV below E_F in the presence of graphene. This is in agreement with previous studies[22,34] for graphene on Cu(111) and can be explained by charge transfer from the Cu surface state to graphene contributing to the observed n-type doping. Instead, for graphene on oxidized Cu(111), the surface state is absent due to the presence of the surface oxide layer on top of Cu(111). The ARPES measurements therefore demonstrate that graphene grown directly on copper oxide is electronically decoupled from the substrate and exhibits comparable properties as freestanding graphene.

Our results show that the commonly held belief that the catalytic activity of the copper oxide for graphene growth is low needs to be reconsidered and that CVD growth on metal oxides surfaces is a promising route for the fabrication of graphene, as well as of graphene nanostructures, on high-k dielectric substrates via industrially scalable and versatile methods.

Indeed, our experiments show that high-quality freestanding graphene can be grown directly on an oxidized copper surface. The possibility of graphene growth on a high k-dielectric copper oxide surface, while preserving a freestanding-like graphene band structure, has great implications for the development of graphene-based electronics.

■ ASSOCIATED CONTENT

Supporting Information

Methods, additional STM images, and LEED analysis. This material is available free of charge via the Internet at http://pubs.acs.org.

■ AUTHOR INFORMATION

Corresponding Authors

*E-mail: (M.S.) m.a.stohr@rug.nl.
*E-mail: (S.G.) s.gottardi@rug.nl.

Present Addresses

(L.B.) Physikalisches Institut, Westfälische Wilhelms-Universität, Wilhelm-Klemm Straße 10, 48149 Münster, Germany.
(O.I.) National Institute for Nanotechnology, University of Alberta 11421, Saskatchewan Dr., T6G 2M9 Edmonton AB, Canada.
(M.Y.) Helmholtz-Zentrum Berlin für Materialien und Energie, Albert-Einstein-Strasse 15, 12489 Berlin, Germany.

Author Contributions

The manuscript was written through contributions of all authors. S.G., K.M., L.B., T.A.P., M.Y., and A.B. performed the ARPES measurements at synchrotron Trieste. S.G., J.C.M.L., and K.M. performed the STM and LEED experiments. S.G. and L.B. grew the graphene. J.B. performed the DFT calculations. S.G., K.M., J.C.M.L., L.B., and O.I. analyzed the data. S.G., P.R. and M.S. conceived the study. S.G., K.M., P.R., and M.S. cowrote the paper. All authors have given approval to the final version of the manuscript.

Notes

The authors declare no competing financial interest.

■ ACKNOWLEDGMENTS

We thank Fei Song, Victor Kandyba, Wesley R. Browne and Luc Venema for their help during the experiments as well as for discussions. This work was supported by the Foundation for Fundamental Research on Matter (FOM), part of The Netherlands Organization for Scientific Research (NWO), by the European Research Council (ERC-2012-StG 307760-SURFPRO), and by NWO (Chemical Sciences, VIDI-Grant 700.10.424 and VENI-Grant 722.012.010).

■ REFERENCES

(1) Castro Neto, H.; Guinea, F.; Peres, N. M. R.; Novoselov, K. S.; Geim, A. K. *Rev. Mod. Phys.* **2009**, *81*, 109−162.
(2) Geim, A. K. *Science* **2009**, *324*, 1530.
(3) Schwierz, F. *Nat. Nanotechnol.* **2010**, *5*, 487−496.
(4) Han, S.-J.; Garcia, A. V.; Oida, S.; Jenkins, K. A.; Haensch, W. *Nat. Commun.* **2014**, *5*, 3086.
(5) Voloshina, E.; Dedkov, Y. *Phys. Chem. Chem. Phys.* **2012**, *14*, 13502−13514.
(6) Batzill, M. *Surf. Sci. Rep.* **2012**, *67*, 83−115.
(7) Mattevi, C.; Kim, H.; Chhowalla, M. *J. Mater. Chem.* **2011**, *21*, 3324.

DOI: 10.1021/nl5036463
Nano Lett. 2015, 15, 917−922

(8) Rümmeli, M. H.; Bachmatiuk, A.; Scott, A.; Börrnert, F.; Warner, J. H.; Hoffman, V.; Lin, J.-H.; Cuniberti, G.; Büchner, B. *ACS Nano* **2010**, *4*, 4206.
(9) Hwang, J.; Kim, M.; Campbell, D.; Alsalman, H. A.; Kwak, J. Y.; Shivaraman, S.; Woll, A. R.; Singh, A. K.; Hennig, R. G.; Gorantla, S.; Rümmeli, M. H.; Spencer, M. G. *ACS Nano* **2013**, *7*, 385.
(10) Sun, J.; Gao, T.; Song, X.; Zhao, Y.; Lin, Y.; Wang, H.; Ma, D.; Chen, Y.; Xiang, W.; Wang, J.; Zhang, Y.; Liu, Z. *J. Am. Chem. Soc.* **2014**, *136*, 6574.
(11) Reckinger, N.; Hooijdonk, E. V.; Joucken, F.; Tyurnina, A. V.; Lucas, S.; Colomer, J.-F. *Nano Res.* **2014**, *7*, 154.
(12) Robinson, Z. R.; Ong, E. W.; Mowll, T. R.; Tyagi, P.; Gaskill, D. K.; Geisler, H.; Ventrice, Carl A. *J. Phys. Chem. C* **2013**, *117*, 23919.
(13) Emtsev, K. V.; Bostwick, A.; Horn, K.; Jobst, J.; Kellogg, G. L.; Ley, L.; McChesney, J. L.; Ohta, T.; Reshanov, S. A.; Röhrl, J.; Rotenberg, E.; Schmid, A. K.; Waldmann, D.; Weber, H. B.; Seyller, T. *Nat. Mater.* **2009**, *8*, 203.
(14) Tejeda, A.; Taleb-Ibrahimi, A.; de Heer, W.; Berger, C.; Conrad, E. H. *New J. Phys.* **2012**, *14*, 125007.
(15) Ristein, J.; Mammadov, S.; Seyller, T. *Phys. Rev. Lett.* **2012**, *108*, 246104.
(16) Varykhalov, A.; Sánchez-Barriga, J.; Shikin, A. M.; Biswas, C.; Vescovo, E.; Rybkin, A.; Marchenko, D.; Rader, O. *Phys. Rev. Lett.* **2008**, *101*, 157601.
(17) Grånäs, E.; Knudsen, J.; Schröder, U. A.; Gerber, T.; Busse, C.; Arman, M. A.; Schulte, K.; Andersen, J. N.; Michely, T. *ACS Nano* **2012**, *6*, 9951.
(18) Lizzit, S.; Larciprete, R.; Lacovig, P.; Dalmiglio, M.; Orlando, F.; Baraldi, A.; Gammelgaard, L.; Barreto, L.; Bianchi, M.; Perkins, E.; Hofmann, P. *Nano Lett.* **2012**, *12*, 4503.
(19) Ismach, A.; Druzgalski, C.; Penwell, S.; Schwartzberg, A.; Zheng, M.; Javey, A.; Bokor, J.; Zhang, Y. *Nano Lett.* **2010**, *10*, 1542.
(20) Zabeti, M.; Wan Daud, W. M. A.; Aroua, M. K. *Fuel Process. Technol.* **2009**, *90*, 770−777.
(21) Bansal, T.; Durcan, C. A.; Jain, N.; Jacobs-Gedrim, R. B.; Xu, Y.; Yu, B. *Carbon* **2013**, *55*, 168.
(22) Jeon, C.; Hwang, H.-N.; Lee, W.-G.; Jung, Y. G.; Kim, K. S.; Park, C.-Y.; Hwang, C.-C. *Nanoscale* **2013**, *5*, 8210.
(23) Zhou, F.; Li, Z.; Shenoy, G. J.; Li, L.; Liu, H. *ACS Nano* **2013**, *7*, 6939−6947.
(24) Kidambi, P. R.; Bayer, B. C.; Blume, R.; Wang, Z.-J.; Baehtz, C.; Weatherup, R. S.; Willinger, M.-G.; Schloegl, R.; Hofmann, S. *Nano Lett.* **2013**, *13*, 4769.
(25) Wlasny, I.; Dabrowski, P.; Rogala, M.; Kowalczyk, P. J.; Pasternak, I.; Strupinski, W.; Baranowski, J. M.; Klusek, Z. *Appl. Phys. Lett.* **2013**, *102*, 111601.
(26) Lu, A.-Y.; Wei, S.-Y.; Wu, C.-Y.; Hernandez, Y.; Chen, T.-Y.; Liu, T.-H.; Pao, C.-W.; Chen, F.-R.; Li, L.-J.; Juang, Z.-Y. *RSC Adv.* **2012**, *2*, 3008.
(27) Zhou, H.; Yu, W. J.; Liu, L.; Cheng, R.; Chen, Y.; Huang, X.; Liu, Y.; Wang, Y.; Huang, Y.; Duan, X. *Nat. Commun.* **2013**, *4*, 2096.
(28) Hao, Y.; Bharathi, M. S.; Wang, L.; Liu, Y.; Chen, H.; Nie, S.; Wang, X.; Chou, H.; Tan, C.; Fallahazad, B.; Ramanarayan, H.; Magnuson, C. W.; Tutuc, E.; Yakobson, B. I.; McCarty, K. F.; Zhang, Y.-W.; Kim, P.; Hone, J.; Colombo, L.; Ruoff, R. S. *Science* **2013**, *342*, 720.
(29) Wood, J. D.; Schmucker, S. W.; Lyons, A. S.; Pop, E.; Lyding, J. W. *Nano Lett.* **2011**, *11*, 4547−4554.
(30) Gao, L.; Guest, J. R.; Guisinger, N. P. *Nano Lett.* **2010**, *10*, 3512−3516.
(31) Soon, A.; Todorova, M.; Delley, B.; Stampfl, C. *Surf. Sci.* **2007**, *601*, 5809−5813.
(32) Onsten, A.; Göthelid, M.; Karlsson, U. O. *Surf. Sci.* **2009**, *603*, 257−264.
(33) Choi, J.-H.; Li, Z.; Cui, P.; Fan, X.; Zhang, H.; Zeng, C.; Zhang, Z. *Sci. Rep.* **2013**, DOI: 10.1038/srep01925.
(34) Khomyakov, P. A.; Giovannetti, G.; Rusu, P. C.; Brocks, G.; van den Brink, J.; Kelly, P. J. *Phys. Rev. B* **2009**, *79*, 195425.
(35) Walter, A. L.; Nie, S.; Bostwick, A.; Kim, K. S.; Moreschini, L.; Chang, Y. J.; Innocenti, D.; Horn, K.; McCarty, K. F.; Rotenberg, E. *Phys. Rev. B* **2011**, *84*, 195443.

DOI: 10.1021/nl5036463
Nano Lett. 2015, 15, 917−922